

## Accepted Manuscript

Type II shell evolution in  $A = 70$  isobars from the  $N \geq 40$  island of inversion

A.I. Morales, G. Benzoni, H. Watanabe, Y. Tsunoda, T. Otsuka et al.

PII: S0370-2693(16)30763-8  
DOI: <http://dx.doi.org/10.1016/j.physletb.2016.12.025>  
Reference: PLB 32491

To appear in: *Physics Letters B*

Received date: 8 August 2016  
Revised date: 15 November 2016  
Accepted date: 8 December 2016

Please cite this article in press as: A.I. Morales et al., Type II shell evolution in  $A = 70$  isobars from the  $N \geq 40$  island of inversion, *Phys. Lett. B* (2016), <http://dx.doi.org/10.1016/j.physletb.2016.12.025>

This is a PDF file of an unedited manuscript that has been accepted for publication. As a service to our customers we are providing this early version of the manuscript. The manuscript will undergo copyediting, typesetting, and review of the resulting proof before it is published in its final form. Please note that during the production process errors may be discovered which could affect the content, and all legal disclaimers that apply to the journal pertain.



Type II shell evolution in  $A = 70$  isobars from the  $N \geq 40$  island of inversion

A.I. Morales<sup>a,b,\*</sup>, G. Benzioni<sup>a</sup>, H. Watanabe<sup>c,d</sup>, Y. Tsunoda<sup>e</sup>, T. Otsuka<sup>f,g,h</sup>, S. Nishimura<sup>d</sup>, F. Browne<sup>i,d</sup>, R. Daido<sup>j</sup>, P. Doornenbal<sup>d</sup>, Y. Fang<sup>j</sup>, G. Lorusso<sup>d</sup>, Z. Patel<sup>k,d</sup>, S. Rice<sup>k,d</sup>, L. Sinclair<sup>l,d</sup>, P.-A. Söderström<sup>d</sup>, T. Sumikama<sup>d</sup>, J. Wu<sup>d</sup>, Z.Y. Xu<sup>f,d</sup>, A. Yagi<sup>j</sup>, R. Yokoyama<sup>f</sup>, H. Baba<sup>d</sup>, R. Avigo<sup>a,b</sup>, F.L. Bello Garrote<sup>n</sup>, N. Blasi<sup>a</sup>, A. Bracco<sup>a,b</sup>, F. Camera<sup>a,b</sup>, S. Ceruti<sup>a,b</sup>, F.C.L. Crespi<sup>a,b</sup>, G. de Angelis<sup>o</sup>, M.-C. Delattre<sup>p</sup>, Zs. Dombradi<sup>q</sup>, A. Gottardo<sup>o</sup>, T. Isobe<sup>d</sup>, I. Kojouharov<sup>r</sup>, N. Kurz<sup>r</sup>, I. Kuti<sup>q</sup>, K. Matsui<sup>f</sup>, B. Melon<sup>s</sup>, D. Mengoni<sup>t,u</sup>, T. Miyazaki<sup>f</sup>, V. Modamio-Hoybjør<sup>o</sup>, S. Momiyama<sup>f</sup>, D.R. Napoli<sup>o</sup>, M. Niikura<sup>f</sup>, R. Orlandi<sup>h,v</sup>, H. Sakurai<sup>d,f</sup>, E. Sahin<sup>n</sup>, D. Sohler<sup>d</sup>, H. Schaffner<sup>r</sup>, R. Taniuchi<sup>f</sup>, J. Taprogge<sup>w,x</sup>, Zs. Vajta<sup>q</sup>, J.J. Valiente-Dobón<sup>o</sup>, O. Wieland<sup>a</sup>, M. Yalcinkaya<sup>y</sup>

<sup>a</sup>Istituto Nazionale di Fisica Nucleare, Sezione di Milano, Via Celoria 16, 20133 Milano, Italy

<sup>b</sup>Dipartimento di Fisica dell'Università degli Studi di Milano, Via Celoria 16, 20133 Milano, Italy

<sup>c</sup>IRCNPC, School of Physics and Nuclear Energy Engineering, Beihang University, Beijing 100191, China

<sup>d</sup>RIKEN Nishina Center, 2-1 Hirosawa, Wako, Saitama 351-0198, Japan

<sup>e</sup>Center for Nuclear Study, The University of Tokyo, Bunkyo-ku, 113-0033 Tokyo, Japan

<sup>f</sup>Department of Physics, The University of Tokyo, Bunkyo-ku, 113-0033 Tokyo, Japan

<sup>g</sup>National Superconducting Cyclotron Laboratory, Michigan State University, East Lansing, MI 48824, USA

<sup>h</sup>Instituut voor Kern- en Stralingsfysica, Katholieke Universiteit Leuven, B-3001 Leuven, Belgium

<sup>i</sup>School of Computing, Engineering and Mathematics, University of Brighton, Brighton, United Kingdom

<sup>j</sup>Department of Physics, Osaka University, Osaka 560-0043 Toyonaka, Japan

<sup>k</sup>Department of Physics, University of Surrey, Guildford GU2 7XH, United Kingdom

<sup>l</sup>Department of Physics, University of York, Heslington, York YO10 5DD, United Kingdom

<sup>m</sup>Department of Physics, Tohoku University, Miyagi 980-8578, Japan

<sup>n</sup>Department of Physics, University of Oslo, N-0316 Oslo, Norway

<sup>o</sup>Istituto Nazionale di Fisica Nucleare, Laboratori Nazionali di Legnaro, I-35020 Legnaro, Italy

<sup>p</sup>IPNO Orsay, 91400 Orsay, France

<sup>q</sup>MTA Atomki, H-4001 Debrecen, Hungary

<sup>r</sup>GSI, Planckstrasse 1, D-64291 Darmstadt, Germany

<sup>s</sup>INFN Sezione di Firenze, I-50019 Firenze, Italy

<sup>t</sup>Dipartimento di Fisica dell'Università degli Studi di Padova, I-35131 Padova, Italy

<sup>u</sup>Istituto Nazionale di Fisica Nucleare, Sezione di Padova, I-35131 Padova, Italy

<sup>v</sup>Advanced Science Research Center, JAEA, Tokai, Ibaraki 319-1195, Japan

<sup>w</sup>Instituto de Estructura de la Materia, CSIC, E-28006 Madrid, Spain

<sup>x</sup>Departamento de Física teórica, Universidad Autónoma de Madrid, E-28049 Madrid, Spain

<sup>y</sup>Department of Physics, Istanbul University, 34134 Istanbul, Turkey

---

**Abstract**

The level structures of  $^{70}\text{Co}$  and  $^{70}\text{Ni}$ , populated from the  $\beta$  decay of  $^{70}\text{Fe}$ , have been investigated using  $\beta$ -delayed  $\gamma$ -ray spectroscopy following in-flight fission of a  $^{238}\text{U}$  beam. The experimental results are compared to Monte-Carlo Shell-Model calculations including the  $pf + g_{9/2} + d_{5/2}$  orbitals. The strong population of a  $(1^+)$  state at 274 keV in  $^{70}\text{Co}$  is at variance with the expected excitation energy of  $\sim 1$  MeV from near spherical single-particle estimates. This observation indicates a dominance of prolate-deformed intruder configurations in the low-lying levels, which coexist with the normal near spherical states. It is shown that the  $\beta$  decay of the neutron-rich  $A=70$  isobars from the new island of inversion to the  $Z=28$  closed-shell regime progresses in accordance with a newly reported type of shell evolution, the so-called Type II, which involves many particle-hole excitations across energy gaps.

**Keywords:**

PACS: 23.40.-s, 29.30.Kv, 23.20.Lv, 21.60.Cs

---

\*Corresponding author. Current affiliation: IFIC, CSIC-Universitat de València, València, Spain  
 Email address: Ana.Morales@ific.uv.es. (A.I. Morales)

In exotic nuclei, which have an increasingly unbalanced number of neutrons ( $N$ ) and protons ( $Z$ ), new aspects, such as neutron-halo or skin structures [1, 2],

magicity loss [3, 4, 5, 6], and new magic numbers [7, 8, 9, 10, 11, 12, 13] have been discovered. These findings have provided pivotal information on single-particle energies and the resultant shell structure far from stability, helping to better understand the role of the tensor, spin-orbit, central, and three-body components of the nucleon-nucleon interaction [14, 15].

The variation of the proton or neutron number is a longstanding recognized cause of shell evolution, yet particular particle-hole excitations in exotic nuclei have shown to alter significantly the shell structure owing to the monopole properties of the central and tensor forces [16, 17]. This is a new, almost unexplored microscopic mechanism of shell evolution (called Type II) that is to be distinguished from the better known shell evolution due to varying neutron or proton number (called Type I) [18, 19].

Shape-transitional phenomena are indicators of alterations in the normal-order configuration of protons and neutrons. For exotic nuclei, they may prelude the discovery of new nuclear regions in which the ground states are dominated by deformed intruder configurations, the so-called “islands of inversion” [20, 21, 22]. Similarly to the  $N = 20$  deformation region in the vicinity of  $^{32}\text{Mg}$ , the abrupt fall of the  $2_1^+$  state in the  $N = 40$  isotones, from 2034 keV in  $^{68}\text{Ni}$  to 574 keV in  $^{66}\text{Fe}$  and 430 keV in  $^{64}\text{Cr}$  [23], indicates an increase of collectivity. The fact that these nuclei are well deformed has been confirmed in a Coulomb excitation experiment at intermediate energy [24]. Later systematic studies of  $2_1^+$  and  $4_1^+$  states in  $^{70}\text{Fe}$ ,  $^{72}\text{Fe}$ , and  $^{66}\text{Cr}$  have revealed that the new island of inversion spreads beyond  $N=40$  [25, 26]. In this context, the discovery of new deformed structures in neighboring nuclei is important to better model the deformation-driving forces approaching the  $N = 50$  shell closure.

Shape transitions can also take place with excitation energy or angular momentum, leading to the coexistence of different shapes within the same nucleus [27]. An exemplary case is  $^{68}\text{Ni}$ , which has a  $j$ - $j$  (spin-orbit) closed shell at  $Z = 28$  and a  $L$ - $S$  (harmonic-oscillator) shell closure at  $N = 40$ . In this nucleus three  $0^+$  states below 3 MeV are related to spherical, prolate, and oblate shapes [18, 28, 29, 30]. In  $^{70}\text{Ni}$ , a second  $0^+$  level has recently been observed at a lower excitation energy than in  $^{68}\text{Ni}$  [31], consistently with a prediction of a deeper local minimum at prolate deformation [18]. In fact, the advanced Monte Carlo Shell-Model (MCSM) calculations [18] have indicated that a combined effect of the proton-neutron tensor force and changes of major configurations is crucial for driving and stabilizing the shape coexistence in the neutron-rich Ni isotopes, as re-

ferred to as Type II shell evolution [19] in contrast to the more conventional Type I shell evolution [11].

The present work exploits the selectivity inherent to the  $\beta$  decay to populate spherical and deformed structures in the neutron-rich  $A = 70$  isobars  $^{70}\text{Co}_{43}$  and  $^{70}\text{Ni}_{42}$ . For  $^{70}\text{Co}$ , Mueller et al. [28] identified two long-lived levels at low and high spins, both of which decay to excited states in  $^{70}\text{Ni}$ . Here, the low-spin state of  $^{70}\text{Co}$  is isolated in the  $\beta$  decay of  $^{70}\text{Fe}_{44}$ , which was previously reported to lie inside the  $N \geq 40$  island of inversion [26]. Selection rules of the  $\beta$  decay process allow for the population of low-spin states in  $^{70}\text{Co}$  while high spin isomeric states in  $^{70}\text{Co}$  could not be effectively populated, as suggested by [28, 32]. Results are compared to MCSM calculations, which predict the inversion of the intruder prolate structure with the normal near-spherical configuration in  $^{70}\text{Co}$ .

The experiment was performed at the Radioactive Isotope Beam Factory (RIBF) in RIKEN, Japan. A  $^{238}\text{U}$  primary beam at 345 MeV/nucleon, with an average intensity of 10 pnA, collided onto a Be target of 3 mm thickness. Fission fragments with  $A \sim 70$  were separated and identified in flight in the BigRIPS spectrometer through the  $\Delta E$ - $B\rho$ -TOF method [34], using position, time, and energy-loss detectors at the focal planes for the measurement of the mass-to-charge ratio  $A/Q$  and the atomic number  $Z$ . The cocktail beam was implanted in the Wide-range Active Silicon Strip Stopper Array for Beta and ion detection (WAS3ABi) [35]. About  $1.8 \times 10^5$  nuclei of  $^{70}\text{Fe}$  were registered in WAS3ABi.

WAS3ABi consisted of a compact row of 5 highly pixelated double-sided silicon strip detectors of dimensions  $60 \times 40 \times 1 \text{ mm}^3$ , with 2400 pixels of  $1 \text{ mm}^2$  pitch each. The energy, position, and time of implanted nuclei and electrons were recorded in WAS3ABi. These information were used offline to correlate them through their positions and times. The  $\beta$ -decay half-lives of the implanted nuclei and their decay successors were determined from these correlations. Resulting values (61.4(7) ms for  $^{70}\text{Fe}$  and 508(7) ms for the low-spin  $\beta$ -decaying state of  $^{70}\text{Ni}$ ) are in reasonable agreement with previous measurements [28, 36, 37, 31]. Energy and time of coincident  $\gamma$  rays were obtained with the EURICA  $\gamma$ -ray spectrometer [38], made of 12 7-element HPGe cluster detectors with an addback efficiency of 11% at 662 keV. More details on the geometry of the setup and analysis procedure are published in Refs. [25, 39, 40, 41].

The level structure of the decay successors was investigated through high-precision  $\beta$ -delayed  $\gamma$  spectroscopy. Correlation conditions consisted in defining

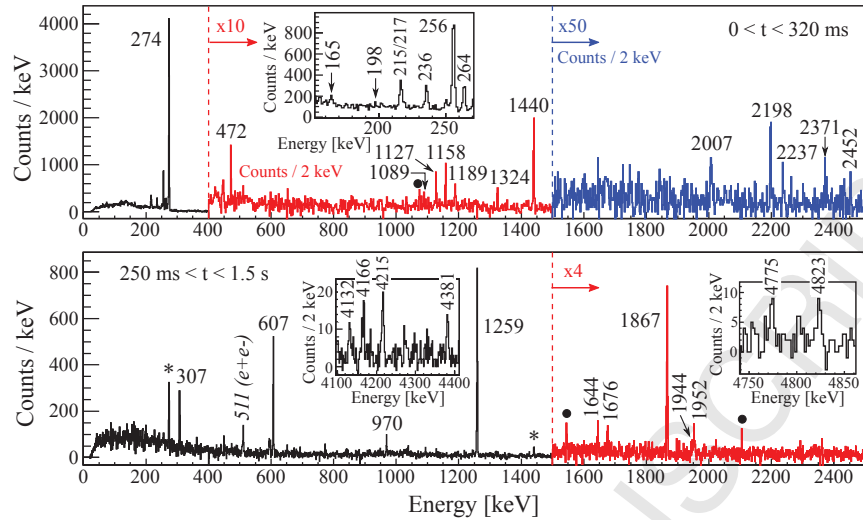


Figure 1: (Color on line) Delayed  $\gamma$  spectra following  $\beta$  decay of  $^{70}\text{Fe}$ . The time intervals 0-320 ms (top) and 250-1500 ms (bottom) are selected to enhance  $\gamma$  rays in  $^{70}\text{Co}$  and  $^{70}\text{Ni}$ , respectively. Transitions placed in the level schemes are labeled by their energies, unplaced  $\gamma$  rays are marked by circles, and transitions assigned to the progenitor are indicated by asterisks. Long-living background components have been subtracted. Inset panels: Parts of spectra zoomed in on energy regions where weak  $\gamma$  rays are observed.

the time interval (typically corresponding to five half-life periods), the distance between implanted ions and  $\beta$  electrons (defined as 3 mm based on electron mean-path considerations) and establishing a coincidence time window between  $\beta$  electrons and  $\gamma$  rays of 200 ns.

Figure 1 shows  $\gamma$ -ray energy spectra measured in delayed coincidence with  $\beta$  electrons registered within 0-320 ms (top) and 250-1500 ms (bottom) after the implantation of  $^{70}\text{Fe}$  ions. These two time windows are selected to enhance the  $\gamma$  rays following the decays  $^{70}\text{Fe} \rightarrow ^{70}\text{Co}$  and  $^{70}\text{Co} \rightarrow ^{70}\text{Ni}$ , respectively. For  $^{70}\text{Co}$ , only three  $\gamma$  transitions at 156, 164, and 273 keV were previously reported [32, 37]. In the present work, a total of 19 transitions have been placed in the level scheme of  $^{70}\text{Co}$  after analyzing their coincidence relations and energy matchings (see Fig. 2).

In the granddaughter nucleus  $^{70}\text{Ni}$  17 transitions are identified, about half of which are reported in Refs. [42, 31]. The level scheme of  $^{70}\text{Ni}$  is also shown in Fig. 2. Transitions shown as dashed lines are placed in the level scheme based only on energy-matching constraints but not on  $\gamma$ - $\gamma$  coincidence relations.

Apparent  $\beta$  feedings and calculated  $\log ft$  values are reported on the left side of the level schemes. They must be considered as upper and lower limits, respectively, due to possible missed feeding from higher-lying states.

In  $^{70}\text{Co}$ , the strong  $\beta$  feeding to the states at 274 and 1696 keV indicates the occurrence of allowed Gamow-Teller transitions from the  $0^+$  ground state of  $^{70}\text{Fe}$ .

Based on this, we tentatively assign them spin and parity ( $1^+$ ). It is to note that the low-lying levels of  $^{70}\text{Co}$  will have negative parity as a result of the coupling of a single proton hole in the  $\pi f_{7/2}$  orbital to the unpaired  $\nu g_{9/2}$  neutron, if these orbitals are well isolated from the adjacent sub-shells with the presence of sizable spherical shell gaps at  $Z = 20, 28$  and  $N = 40, 50$ . Meanwhile, the first spherical  $1^+$  state will arise from the  $\pi f_{7/2} \otimes \nu f_{5/2}$  multiplet. Its energy is expected to be around 1 MeV based on the energy difference between the  $(9/2^+)$  ground state and the  $(5/2^-)$  level in the  $N = 43$  isotone  $^{71}\text{Ni}$  [43], which are interpreted in terms of a single neutron in the  $g_{9/2}$  and  $f_{5/2}$  orbitals, respectively.

For a deformed nucleus, the  $2j + 1$  degeneracy of the spherical orbitals is solved with respect to the projection of the single-particle angular momentum  $j$  on the symmetry axis,  $\Omega$ . The deformed single-particle levels are labeled by the asymptotic quantum number  $\Omega^\pi [Nn_z\Lambda]$  in the Nilsson model [44]. In the odd-even isotopes  $^{65}\text{Co}_{38}$  and  $^{67}\text{Co}_{40}$ , the respective lowest-lying  $(1/2^-)$  states at 1095 and 492 keV are ascribed to a downslipping intruder  $1/2^- [321]$  proton orbit [45], indicating an evolution of the nuclear shape towards prolate deformation. In the neighboring odd-odd isotopes, a low-lying deformed  $1^+$  state most likely involves a neutron in the  $1/2^- [301]$  orbit coupled to the aforementioned proton intruder state [46, 47]. Thus, the observation of the  $1^+$  state at 274 keV in  $^{70}\text{Co}$  provides evidence for the

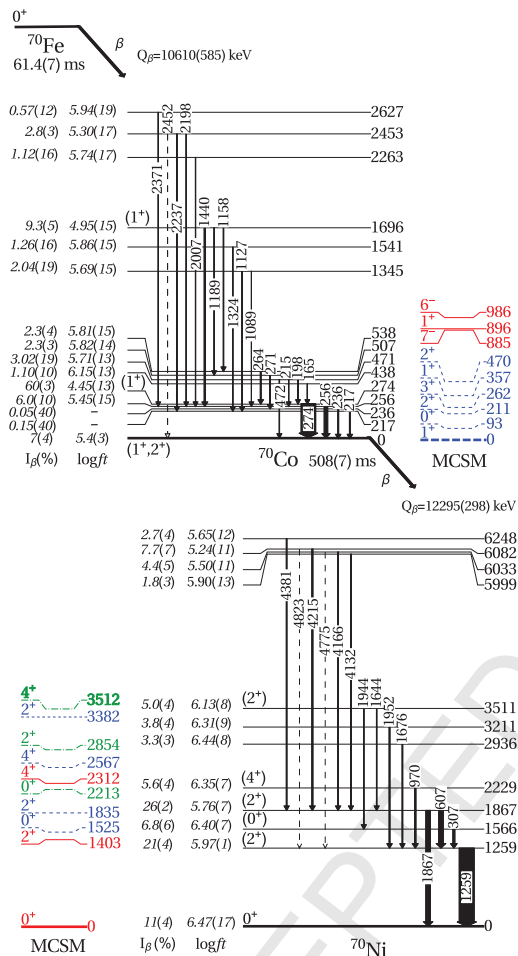


Figure 2: (Color on line) Experimental and calculated level schemes of the decay  $^{70}\text{Fe} \rightarrow ^{70}\text{Co} \rightarrow ^{70}\text{Ni}$ . Arrow widths are proportional to transition intensities. Transitions shown by dashed arrows are placed based only on energy-matching constraints. Apparent  $\beta$  feedings ( $I_\beta$ ) and  $\log ft$  values (calculated assuming the lowest-lying level as the ground state) are shown. MCSM states predicted to be nearly spherical or slightly prolate-deformed ( $\beta_2 \leq 0.2$ ) are indicated in solid red, strongly prolate-deformed ( $\beta_2 > 0.2$ ) in dashed blue, and oblate-deformed ( $\beta_2 \sim -0.13$ ) in dotted-dashed green.  $Q_\beta$  values are taken from [33].

existence of a deformed-shape configuration. Theoretically, this deformed low-lying  $1^+$  state of  $^{70}\text{Co}$  is a consequence of many particle-hole excitations across the  $Z=28$  and  $N=40$  shell gaps induced by effect of Type II shell evolution [19]. Conversely, it may not arise in a simple single-particle picture based on a spherical shape.

The experimental  $\beta$ -decay level schemes are interpreted with the help of the MCSM calculations based on the A3DA Hamiltonian [49]. The model space includes the full  $pf$  shell and the  $0g_{9/2}$ ,  $1d_{5/2}$  orbitals for both protons and neutrons. The calculated levels are shown in Fig. 2. The results predict that the low-lying states of  $^{70}\text{Co}$ , including a  $J^\pi = 1^+$  level at 357 keV and the ground state, are dominated by strongly prolate configurations with deformation parameter  $\beta_2 \sim 0.27$ . States characterized by small deformation,  $\beta_2 \sim 0.15$ , appear at about 900 keV and above. The theoretical  $B(GT; 0^+ \rightarrow 1^+)$  and the corresponding  $\log ft$  values, evaluated as  $ft = 6147 / [(g_A/g_V)^2 B(GT)]$  with coupling constant ratio  $g_A/g_V = -1.266$  [50], for the  $^{70}\text{Fe} \rightarrow ^{70}\text{Co}$  decay are listed in the first column of Table 1, while those referring to the  $^{70}\text{Co} \rightarrow ^{70}\text{Ni}$  are listed in the second, third and fourth columns. The calculation indicates an abundance of population of two excited  $1^+$  levels, along with a highly hindered  $\beta$  feeding to the deformed  $1^+$  ground state. This prediction is consistent with both the observed decay pattern to the states at 274 and 1696 keV, and the weak population of the low-spin  $\beta$ -decaying state, which can be understood as the ground state in the MCSM interpretation.

Figure 3 exhibits potential energy surface (PES) plots for  $^{70}\text{Fe}$  and  $^{70}\text{Co}$  in terms of the quadrupole moments  $Q_0$  and  $Q_2$  calculated by the constrained Hartree-Fock (CHF) method for the current Hamiltonian. The location and size of circles on the PESs represent the intrinsic shape of each MCSM basis state and its significance in the eigenstate being considered, respectively, as called  $T$ -plot [18]. It can be seen in Fig. 3(a) that for the  $0^+$  ground state of  $^{70}\text{Fe}$  many circles are distributed in the local minimum of moderate prolate deformation with  $Q_0 \sim 150 \text{ fm}^2$ . For  $^{70}\text{Co}$ , the  $1^+_{1,2}$  states in Figs. 3(b) and 3(c) exhibit almost identical distribution around  $Q_0 = 175 \text{ fm}^2$ , while the circles of the  $1^+_3$  state in Fig. 3(d) spread on a shallow potential well at  $Q_0 \sim 100 \text{ fm}^2$ . Thus, the degree of quadrupole deformation of the  $^{70}\text{Fe}$  ground state is in between those for the modestly deformed  $1^+_3$  and the largely deformed  $1^+_{1,2}$  states of  $^{70}\text{Co}$ .

The occupancies of protons and neutrons in the active shell-model orbitals calculated for the three  $1^+$  states



Table 1:  $B(GT)$  (multiplied by a standard quenching factor of  $0.74^2$  [48]) and  $\log ft$  values calculated by the MCSM calculations for selected levels in the  $\beta$  decay of  $^{70}\text{Fe}$  and  $^{70}\text{Co}$ .  $J_p^\pi$  and  $J_d^\pi$  denote the spin and parity of the parent and daughter states, respectively.

$^{70}\text{Fe} \rightarrow ^{70}\text{Co}$				$^{70}\text{Co} \rightarrow ^{70}\text{Ni}$				$^{70}\text{Co} \rightarrow ^{70}\text{Ni}$				$^{70}\text{Co} \rightarrow ^{70}\text{Ni}$			
$J_p^\pi$	$J_d^\pi$	$B(GT)$	$\log ft$	$J_p^\pi$	$J_d^\pi$	$B(GT)$	$\log ft$	$J_p^\pi$	$J_d^\pi$	$B(GT)$	$\log ft$	$J_p^\pi$	$J_d^\pi$	$B(GT)$	$\log ft$
$0^+$	$1_1^+$	$4 \times 10^{-5}$	7.9	$1_1^+$	$0_1^+$	$3 \times 10^{-6}$	9.2	$2_1^+$	$2_1^+$	$1 \times 10^{-5}$	8.6	$3_1^+$	$2_1^+$	$8 \times 10^{-7}$	9.7
	$1_2^+$	$3.7 \times 10^{-2}$	5.02		$0_2^+$	$6 \times 10^{-5}$	7.8		$2_2^+$	$1.9 \times 10^{-3}$	6.31		$2_2^+$	$1 \times 10^{-4}$	7.5
	$1_3^+$	$1.8 \times 10^{-1}$	4.33		$2_1^+$	$7 \times 10^{-5}$	7.7		$2_3^+$	$9 \times 10^{-5}$	7.6		$2_3^+$	$3 \times 10^{-6}$	9.1
				$2_2^+$	$4.8 \times 10^{-3}$	5.90	$2_4^+$	$1.9 \times 10^{-3}$	6.30	$2_4^+$	$3 \times 10^{-4}$	7.2	$4_1^+$	$1 \times 10^{-5}$	8.4
				$2_3^+$	$1 \times 10^{-6}$	9.4				$4_2^+$	$7.4 \times 10^{-3}$	5.71			
				$2_4^+$	$5.4 \times 10^{-3}$	5.85									

of  $^{70}\text{Co}$  are shown in the top panels of Fig. 4. The configurations of the  $1_{1,2}^+$  states are found to be almost identical, while the  $1_3^+$  state differs from the other two. The wave function of the  $1_3^+$  state consists predominantly of the  $\pi f_{7/2}^{-1} \otimes \nu f_{5/2}^{-1} g_{9/2}^{+4}$  component. Hence, the apparent  $\beta$  feeding measured to the ( $1^+$ ) experimental candidate at 1696 keV can be attributed to the allowed Gamow-Teller transition  $\nu f_{5/2} \rightarrow \pi f_{7/2}$ . On the contrary, the  $1_{1,2}^+$  states mainly involve proton excitations from  $f_{7/2}$  to  $p_{3/2}$  and  $f_{5/2}$ , and neutron excitations from  $f_{5/2}$  and  $p_{1/2}$  to  $g_{9/2}$ . Such multiple particle-hole excitations across the  $Z = 28$  and  $N = 40$  shell gaps (Type II shell evolution) drive the  $1_{1,2}^+$  states towards a strongly prolate-deformed shape, leading to the enhancement of shape coexistence [18, 19]. The observed energy difference between the near spherical ( $1_3^+$ ) candidate and the lowest-lying deformed state is larger than the MCSM prediction by 800 keV. This difference may imply that the isolated prolate local minimum is more stabilized than expected by the model.

Despite very similar occupancies, there is a discrepancy in  $\beta$ -decay strength between the  $1_1^+$  and  $1_2^+$  states of  $^{70}\text{Co}$  (see the left column in Table 1). This can be explained by decomposing the resultant  $B(GT)$  into the Gamow-Teller matrix elements  $M(GT)$ , as illustrated in the bottom panels of Fig. 4: For the  $1_1^+$  state the main (positive)  $\nu p_{1/2} \rightarrow \pi p_{1/2}$  component is almost canceled out by the other components, while the contribution of the  $\nu p_{1/2} \rightarrow \pi p_{3/2}$  transition remains predominant for the  $1_2^+$  state. Furthermore, their nature can be understood based on the deformed single-particle orbitals (DSO) that are obtained by the CHF calculation using the MCSM Hamiltonian<sup>1</sup>. For the energy minimum in the PES of  $^{70}\text{Co}$ , the 27th proton is expected to occupy the second lowest  $|\Omega_p| = 1/2^-$  DSO in the model space. This DSO is dominated by the spherical  $\pi f_{5/2}$  orbit ( $\sim 70\%$ ) rather than  $\pi p_{3/2}$ . The downward trend of the

$|\Omega_p| = 1/2^-$  DSO as the prolate deformation increases is analogous to the  $\pi 1/2^-$  [321] orbital in the Nilsson diagram. Meanwhile, the 43rd neutron occupies the highest  $|\Omega_n| = 1/2^-$  DSO, which is similar to the  $\nu 1/2^-$  [301] Nilsson orbit. The leading component ( $\sim 80\%$ ) of this DSO arises from the  $\nu p_{1/2}$  orbital. From these configurations, deformed bases (Slater determinants) are created with  $|\Omega_p + \Omega_n| = 0^+, 1^+$ . It turns out that about 75% of the original MCSM wave functions of the  $1_{1,2}^+$  states can be reproduced by a linear combination of the angular momentum- and parity-projected ( $J^\pi = 1^+$ ) deformed bases. As seen in Fig. 4, the  $M(GT)$  distribution obtained for the (mixed) deformed bases resembles that of the original MCSM calculation. Therefore, the two prolate  $1^+$  states at low excitation energy in  $^{70}\text{Co}$  can be interpreted as a superposition of the  $|\Omega_p + \Omega_n| = 0^+$  and  $1^+$  deformed bases.

The subsequent  $\beta$  decay to  $^{70}\text{Ni}$  is governed by the large  $\beta$  feeding to the  $2_{1,2}^+$  states, pointing to a  $J^\pi = 1^+, 2^+$ , or  $3^+$  assignment for the long-lived state of  $^{70}\text{Co}$ . According to the MCSM calculations, the  $^{70}\text{Co} \rightarrow ^{70}\text{Ni}$  decay would proceed via a strong transition to the ( $4_2^+$ ) state at 2508 keV [42] if the  $\beta$  decay took place from a deformed  $3_1^+$  level, see the right column in Table 1. Since this is at variance with the present experimental results, a  $J^\pi = 3^+$  assignment is discarded. The calculated  $1_1^+$  and  $2_1^+$  levels of  $^{70}\text{Co}$  decay preferentially to the  $2_2^+$  and  $2_4^+$  states of  $^{70}\text{Ni}$  with small  $\log ft$  values, which are comparable to  $\log ft = 5.76(7)$  and  $6.13(8)$  observed for the ( $2_2^+$ ) and ( $2_4^+$ ) states, respectively (see Fig. 2). These arguments indicate that the  $T_{1/2} = 508$  ms  $\beta$ -decaying state of  $^{70}\text{Co}$  has a spin and parity of  $1^+$  or  $2^+$ .

Experimentally, the ( $2_1^+$ ) state is as strongly populated as the ( $2_2^+$ ) level. The MCSM calculations predict a near spherical shape for the  $0_1^+$  and  $2_1^+$  levels of  $^{70}\text{Ni}$ , while prolate-deformed configurations stabilized by effect of Type II shell evolution dominate its  $0_2^+$  and  $2_{2,4}^+$  levels,

<sup>1</sup>The DSOs used in the current discussion are calculated for  $^{70}\text{Fe}$ .

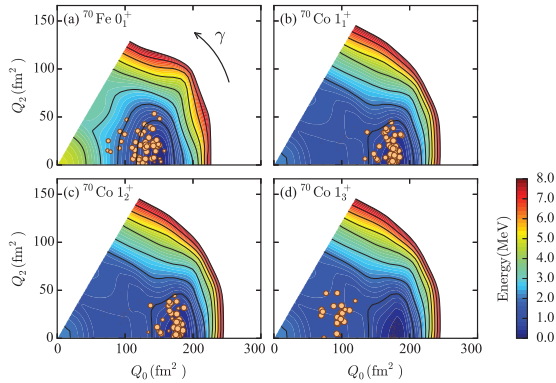


Figure 3: (Color on line) Potential energy surface (PES) plots for (a) the  $0^+$  ground state of  $^{70}\text{Fe}$  and (b)-(d) the  $1^+$  states of  $^{70}\text{Co}$ . See the text for orange circles ( $T$ -plot).

and the low-lying states of  $^{70}\text{Co}$ . Thus, it is natural that the  $(2_2^+)$  level shows a higher feeding ratio than the  $(2_1^+)$  level. A more quantitative analysis, however, needs more precise  $\log ft$  values, as they are obtained presently from observed  $\gamma$ -ray intensities, indicating only lower limits.

In  $^{70}\text{Ni}$ , four new excited states at about 6 MeV are populated with  $\log ft \sim 5.7$  from the low-spin state of  $^{70}\text{Co}$ . They preferentially feed the  $(2_2^+)$  state (see Fig. 2), suggesting a similar deformed structure. These decay patterns can be naively explained using the argument based on the DSO. For  $Q_0 \gtrsim 200 \text{ fm}^2$  corresponding to the prolate local minimum in the PES of  $^{70}\text{Ni}$  (see Fig. 3 in Ref. [18]), the highest  $|\Omega_p| = 1/2^-$  and  $3/2^-$  proton orbitals locate 6 – 7 MeV above the second lowest  $|\Omega_p| = 1/2^-$  orbit, which is included in the deformed  $1_1^+$  configuration in  $^{70}\text{Co}$  as discussed previously. Since the major components of these DSOs are the  $\pi p_{1/2}$  ( $\sim 80\%$ ) and  $\pi p_{3/2}$  ( $\sim 70\%$ ) spherical orbitals, respectively, it is expected that the  $|\Omega_n| = 1/2^-$  neutron can transform to them through strong Gamow-Teller transitions, giving rise to proton two-quasiparticle configurations with  $J^\pi = 0^+, 1^+, 2^+$  around 6 MeV.

In conclusion, the properties of the  $^{70}\text{Fe} \rightarrow ^{70}\text{Co} \rightarrow ^{70}\text{Ni}$  decay chain are interpreted in terms of advanced MCSM calculations. The results provide first evidence of strongly prolate-deformed shapes for the low-lying levels in  $^{70}\text{Co}$ , including the ground state which preferentially decays towards similarly deformed structures in  $^{70}\text{Ni}$ . This decay path can be clearly distinguished from the one passing through nearly spherical levels following the  $\beta$  decay of the high-spin state of  $^{70}\text{Co}$ , as reported in Ref. [31]. Thus, it turns out that the shape coexistence occurs in the  $A = 70$  isobaric chain due

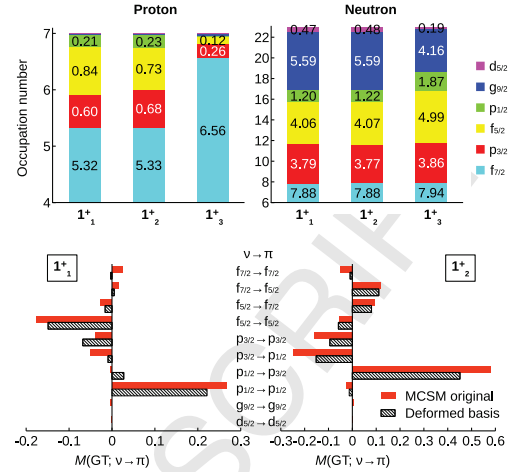


Figure 4: (Color on line) Top: Occupancies of single-particle orbitals in the MCSM calculation for the  $1^+$  levels of  $^{70}\text{Co}$ . Bottom: Gamow-Teller matrix elements for the  $0^+ \rightarrow 1_1^+$  (left) and  $0^+ \rightarrow 1_2^+$  (right) transitions. Filled and shaded bars represent the results of the original MCSM calculation and the deformed bases (see text). The latter are not multiplied by a quenching factor.

to type II shell evolution. A challenge for future radioactive ion-beam facilities will be determining if the deformed-intruder dominance of the ground state is extended to the  $N = 50$  isotones below  $^{78}\text{Ni}$ .

The excellent work of the RIKEN accelerator staff for providing a stable and high intensity  $^{238}\text{U}$  beam is acknowledged. We acknowledge the EUROBALL Owners Committee for the loan of germanium detectors and the PreSpec Collaboration for the readout electronics of the cluster detectors. Part of the WAS3ABi was supported by the Rare Isotope Science Project, which is funded by the Ministry of Science, ICT and Future Planning (MSIP) and National Research Foundation (NRF) of Korea. The MCSM calculations were performed on the K computer at the RIKEN AICS (Project ID: hp150224). This work is co-financed by the European Union and the European Social Fund. Support from Programmi di Ricerca Scientifica di Rilevante Interesse Nazionale (PRIN) number 2001024324.01302, the NuPNET-ERA-NET within the NuPNET GANAS project under grant agreement No.202914, and the European Union within the 7th Framework Program FP7/2007-2013 under grant agreement No. 262010 ENSAR-INDESYS is acknowledged. This work was also financed by the Spanish Ministerio de Ciencia e Innovación under Contracts No. FPA2009-13377-C02 and No. FPA2011-29854-C04, the Hungarian Research Fund OTKA contract numbers K100835 and K106035,

the European Commission through the Marie Curie Actions Contract No. PIEFGA-2001-30096 and by the Japanese JSPS KAKENHI Grants No. 24740188 and No. 25247045.

- [1] I. Tanihata, H. Hamagaki, O. Hashimoto, Y. Shida, N. Yoshikawa, K. Sugimoto, O. Yamakawa, T. Kobayashi, N. Takahashi, *Phys. Rev. Lett.* 55 (1985) 2676.
- [2] P. G. Hansen, B. Jonson, *Europhys. Lett.* 4 (1987) 409.
- [3] C. Détraz, D. Guillemaud, G. Huber, R. Klapisch, M. Langevin, F. Naulin, C. Thibault, L. C. Carraz, F. Touchard, *Phys. Rev. C* 19 (1979) 164.
- [4] E. Caurier, F. Nowacki, A. Poves, J. Retamosa, *Phys. Rev. C* 58 (1998) 2033.
- [5] A. Navin, D. W. Anthony, T. Aumann, T. Baumann, D. Bazin, Y. Blumenfeld, B. A. Brown, T. Glasmacher, P. G. Hansen, R. W. Ibbotson, P. A. Lofy, V. Maddalena, K. Miller, T. Nakamura, B. V. Pritychenko, B. M. Sherrill, E. Spears, M. Steiner, J. A. Tostevin, J. Yurkon, A. Wagner, *Phys. Rev. Lett.* 85 (2000) 266.
- [6] B. Bastin, S. Grévy, D. Sohler, O. Sorlin, Z. Dombrádi, N. L. Achouri, J. C. Angélique, F. Azaiez, D. Baiborodin, R. Borcea, C. Bourgeois, A. Buta, A. Bürger, R. Chapman, J. C. Dalouzy, Z. Dlouhy, A. Drouard, Z. Elekes, S. Franchoo, S. Jacob, B. Laurent, M. Lazar, X. Liang, E. Liénard, J. Mrazek, L. Nalpas, F. Negoita, N. A. Orr, Y. Penionzhkevich, Z. Podolyák, F. Pougheon, P. Roussel-Chomaz, M. G. Saint-Laurent, M. Stanoiu, I. Stefan, F. Nowacki, A. Poves, *Phys. Rev. Lett.* 99 (2007) 022503.
- [7] I. Talmi, I. Unna, *Phys. Rev. Lett.* 4 (1960) 469.
- [8] A. Ozawa, T. Kobayashi, T. Suzuki, K. Yoshida, I. Tanihata, *Phys. Rev. Lett.* 84 (2000) 5493–5495.
- [9] T. Otsuka, R. Fujimoto, Y. Utsuno, B. A. Brown, M. Honma, T. Mizusaki, *Phys. Rev. Lett.* 87 (2001) 082502.
- [10] J. I. Prisciandaro, P. F. Mantica, B. A. Brown, D. W. Anthony, M. W. Cooper, A. Garcia, D. E. Groh, A. Komives, W. Kumarasiri, P. A. Lofy, A. M. Oros-Peusquens, S. L. Tabor, M. Wiedeking, *Physics Letters B* 510 (2001) 17.
- [11] T. Otsuka, T. Suzuki, R. Fujimoto, H. Grawe, Y. Akaishi, *Phys. Rev. Lett.* 95 (2005) 232502.
- [12] R. V. F. Janssens, *Nature* 459 (2009) 1069.
- [13] D. Steppenbeck, et al., *Nature* 502 (2013) 207.
- [14] T. Otsuka, T. Suzuki, M. Honma, Y. Utsuno, N. Tsunoda, K. Tsukiyama, M. Hjorth-Jensen, *Phys. Rev. Lett.* 104 (2010) 012501.
- [15] T. Otsuka, T. Suzuki, J. D. Holt, A. Schwenk, Y. Akaishi, *Phys. Rev. Lett.* 105 (2010) 032501.
- [16] T. Togashi, Y. Tsunoda, T. Otsuka, N. Shimizu, *Phys. Rev. Lett.* 117 (2016) 172502.
- [17] C. Kremer, S. Aslanidou, S. Bassauer, M. Hilcker, A. Krugmann, P. von Neumann-Cosel, T. Otsuka, N. Pietralla, V. Y. Ponomarev, N. Shimizu, M. Singer, G. Steinhilber, T. Togashi, Y. Tsunoda, V. Werner, M. Zweidinger, *Phys. Rev. Lett.* 117 (2016) 172503.
- [18] Y. Tsunoda, T. Otsuka, N. Shimizu, M. Honma, Y. Utsuno, *Phys. Rev. C* 89 (2014) 031301(R).
- [19] T. Otsuka, Y. Tsunoda, *J. Phys. G: Nucl. Part. Phys.* 43 (2016) 024009.
- [20] E. K. Warburton, J. A. Becker, B. A. Brown, *Phys. Rev. C* 41 (1990) 1147.
- [21] K. Wimmer, T. Kröll, R. Krücken, V. Bildstein, R. Gemhäuser, B. Bastin, N. Bree, J. Diriken, P. Van Duppen, M. Huyse, N. Patronis, P. Vermaelen, D. Voulot, J. Van de Walle, F. Wenander, L. M. Fraile, R. Chapman, B. Hadinia, R. Orlandi, J. F. Smith, R. Lutter, P. G. Thirof, M. Labiche, A. Blazhev, M. Kalkühler, P. Reiter, M. Seidlitz, N. Warr, A. O. Macchiavelli, H. B. Jeppesen, E. Fiori, G. Georgiev, G. Schrieder, S. Das Gupta, G. Lo Bianco, S. Nardelli, J. Butterworth, J. Johansen, K. Riisager, *Phys. Rev. Lett.* 105 (2010) 252501.
- [22] C. Force, S. Grévy, L. Gaudefrey, O. Sorlin, L. Cáceres, F. Rotaru, J. Mrazek, N. L. Achouri, J. C. Angélique, F. Azaiez, B. Bastin, R. Borcea, A. Buta, J. M. Daugas, Z. Dlouhy, Z. Dombrádi, F. De Oliveira, F. Negoita, Y. Penionzhkevich, M. G. Saint-Laurent, D. Sohler, M. Stanoiu, I. Stefan, C. Stodel, F. Nowacki, *Phys. Rev. Lett.* 105 (2010) 102501.
- [23] <http://www.nndc.bnl.gov/ensdf/>.
- [24] H. L. Crawford, R. M. Clark, P. Fallon, A. O. Macchiavelli, T. Baugher, D. Bazin, C. W. Beausang, J. S. Berryman, D. L. Bleuel, C. M. Campbell, M. Cromaz, G. de Angelis, A. Gade, R. O. Hughes, I. Y. Lee, S. M. Lenzi, F. Nowacki, S. Paschalidis, M. Petri, A. Poves, A. Ratkiewicz, T. J. Ross, E. Sahin, D. Weishaar, K. Wimmer, R. Winkler, *Phys. Rev. Lett.* 110 (2013) 242701.
- [25] G. Benzoni, A. I. Morales, H. Watanabe, S. Nishimura, L. Coraggio, N. Itaco, A. Gargano, F. Browne, R. Daido, P. Doornenbal, Y. Fang, G. Lorusso, Z. Patel, S. Rice, L. Sinclair, P.-A. Söderström, T. Sumikama, J. Wu, Z. Xu, R. Yokoyama, H. Baba, R. Avigo, F. B. Garrote, N. Blasi, A. Bracco, F. Camera, S. Ceruti, F. Crespi, G. de Angelis, M.-C. Delattre, Z. Dombradi, A. Gottardo, T. Isobe, I. Kuti, K. Matsui, B. Melon, D. Mengoni, T. Miyazaki, V. Modamio-Hoybjor, S. Momiyama, D. Napoli, M. Niikura, R. Orlandi, H. Sakurai, E. Sahin, D. Sohler, R. Taniuchi, J. Taprogge, Z. Vajta, J. Valiente-Dobón, O. Wieland, M. Yalcinkaya, *Phys. Lett. B* 751 (2015) 107.
- [26] C. Santamaria, C. Louchart, A. Obertelli, V. Werner, P. Doornenbal, F. Nowacki, G. Authelet, H. Baba, D. Calvet, F. Château, A. Corsi, A. Delbart, J.-M. Gheller, A. Gillibert, T. Isobe, V. Lapoux, M. Matsushita, S. Momiyama, T. Motobayashi, M. Niikura, H. Otsu, C. Péron, A. Peyaud, E. C. Pollacco, J.-Y. Roussé, H. Sakurai, M. Sasano, Y. Shiga, S. Takeuchi, R. Taniuchi, T. Uesaka, H. Wang, K. Yoneda, F. Browne, L. X. Chung, Z. Dombradi, S. Franchoo, F. Giacoppo, A. Gottardo, K. Hadynska-Klek, Z. Korkulu, S. Koyama, Y. Kubota, J. Lee, M. Lettmann, R. Lozeva, K. Matsui, T. Miyazaki, S. Nishimura, L. Olivier, S. Ota, Z. Patel, N. Pietralla, E. Sahin, C. Shand, P.-A. Söderström, I. Stefan, D. Steppenbeck, T. Sumikama, D. Suzuki, Z. Vajta, J. Wu, Z. Xu, *Phys. Rev. Lett.* 115 (2015) 192501.
- [27] K. Heyde, J. L. Wood, *Rev. Mod. Phys.* 83 (2011) 1467.
- [28] W. F. Mueller, B. Bruyneel, S. Franchoo, M. Huyse, J. Kurpeta, K. Kruglov, Y. Kudryavtsev, N. V. S. V. Prasad, R. Raabe, I. Reusen, P. Van Duppen, J. Van Roosbroeck, L. Vermeeren, L. Weissman, Z. Janas, M. Karny, T. Kszczot, A. Plochocki, K.-L. Kratz, B. Pfeiffer, H. Grawe, U. Köster, P. Thirof, W. B. Walters, *Phys. Rev. C* 61 (2000) 054308.
- [29] S. Suchyta, S. N. Liddick, Y. Tsunoda, T. Otsuka, M. B. Bennett, A. Chemey, M. Honma, N. Larson, C. J. Prokop, S. J. Quinn, N. Shimizu, A. Simon, A. Spyrou, V. Tripathi, Y. Utsuno, J. M. VonMoss, *Phys. Rev. C* 89 (2014) 021301.
- [30] F. Flavigny, D. Pauwels, D. Radulov, I. J. Darby, H. De Witte, J. Diriken, D. V. Fedorov, V. N. Fedosseev, L. M. Fraile, M. Huyse, V. S. Ivanov, U. Köster, B. A. Marsh, T. Otsuka, L. Popescu, R. Raabe, M. D. Seliverstov, N. Shimizu, A. M. Sjödin, Y. Tsunoda, P. Van den Bergh, P. Van Duppen, J. Van de Walle, M. Venhart, W. B. Walters, K. Wimmer, *Phys. Rev. C* 91 (2015) 034310.
- [31] C. J. Prokop, B. P. Crider, S. N. Liddick, A. D. Ayangeakaa, M. P. Carpenter, J. J. Carroll, J. Chen, C. J. Chiara, H. M. David, A. C. Dombos, S. Go, J. Harker, R. V. F. Janssens, N. Larson, T. Lauritsen, R. Lewis, S. J. Quinn, F. Recchia, D. Seweryniak, A. Spyrou, S. Suchyta, W. B. Walters, S. Zhu, *Phys. Rev. C* 92



- (2015) 061302.
- [32] J. M. Daugas, T. Faul, H. Grawe, M. Pfützner, R. Grzywacz, M. Lewitowicz, N. L. Achouri, J. C. Angélique, D. Baiborodin, R. Bentida, R. Béraud, C. Borcea, C. R. Bingham, W. N. Catford, A. Emsallem, G. de France, K. L. Grzywacz, R. C. Lemon, M. J. Lopez Jimenez, F. de Oliveira Santos, P. H. Regan, K. Rykaczewski, J. E. Sauvestre, M. Sawicka, M. Stanoiu, K. Sieja, F. Nowacki, *Phys. Rev. C* 81 (2010) 034304.
- [33] M. Wang, G. Audi, A. Wapstra, F. Kondev, M. MacCormick, X. Xu, B. Pfeiffer, *Chinese Physics C* 36 (2012) 1603.
- [34] N. Fukuda, T. Kubo, T. Ohnishi, N. Inabe, H. Takeda, D. Kameda, H. Suzuki, *Nucl. Instrum. Methods B* 317 (2013) 323.
- [35] S. Nishimura, *Prog. Theor. Exp. Phys.* 03C006.
- [36] J. M. Daugas, I. Matea, J.-P. Delaroche, M. Pfützner, M. Sawicka, F. Becker, G. Bélier, C. R. Bingham, R. Borcea, E. Bouchez, A. Buta, E. Dragulescu, G. Georgiev, J. Giovannozzo, M. Girod, H. Grawe, R. Grzywacz, F. Hammache, F. Ibrahim, M. Lewitowicz, J. Libert, P. Mayet, V. Méot, F. Negroita, F. de Oliveira Santos, O. Perru, O. Roig, K. Rykaczewski, M. G. Saint-Laurent, J. E. Sauvestre, O. Sorlin, M. Stanoiu, I. Stefan, C. Stodel, C. Theisen, D. Verney, J. Żylicz, *Phys. Rev. C* 83 (2011) 054312.
- [37] C. Mazzocchi, R. Surman, R. Grzywacz, J. C. Batchelder, C. R. Bingham, D. Fong, J. H. Hamilton, J. K. Hwang, M. Karny, W. Królas, S. N. Liddick, P. F. Mantica, A. C. Morton, W. F. Mueller, K. P. Rykaczewski, M. Steiner, A. Stolz, J. A. Winger, I. N. Borzov, *Phys. Rev. C* 88 (2013) 064320.
- [38] P.-A. Söderström, S. Nishimura, P. Doornenbal, G. Lorusso, T. Sumikama, H. Watanabe, Z. Xu, H. Baba, F. Browne, S. Go, G. Gey, T. Isobe, H.-S. Jung, G. Kim, Y.-K. Kim, I. Kojouharov, N. Kurz, Y. Kwon, Z. Li, K. Moschner, T. Nakao, H. Nishibata, M. Nishimura, A. Odahara, H. Sakurai, H. Schaffner, T. Shimoda, J. Taprogge, Z. Vajta, V. Werner, J. Wu, A. Yagi, K. Yoshinaga, *NIMB* 317 (2012) 649.
- [39] A. I. Morales, G. Benzoni, H. Watanabe, S. Nishimura, F. Browne, R. Daido, P. Doornenbal, Y. Fang, G. Lorusso, Z. Patel, S. Rice, L. Sinclair, P.-A. Söderström, T. Sumikama, J. Wu, Z. Y. Xu, A. Yagi, R. Yokoyama, H. Baba, R. Avigo, F. L. Bello Garrote, N. Blasi, A. Bracco, F. Camera, S. Ceruti, F. C. L. Crespi, G. de Angelis, M.-C. Delattre, Z. Dombradi, A. Gottardo, T. Isobe, I. Kojouharov, N. Kurz, I. Kuti, K. Matsui, B. Melon, D. Mengoni, T. Miyazaki, V. Modamio-Hoyborg, S. Momiyama, D. R. Napoli, M. Niikura, R. Orlandi, H. Sakurai, E. Sahin, D. Sohler, H. Schaffner, R. Taniuchi, J. Taprogge, Z. Vajta, J. J. Valiente-Dobón, O. Wieland, M. Yalcinkaya, *Phys. Rev. C* 93 (2016) 034328.
- [40] J. Taprogge, A. Jungclauss, H. Grawe, S. Nishimura, P. Doornenbal, G. Lorusso, G. S. Simpson, P.-A. Söderström, T. Sumikama, Z. Y. Xu, H. Baba, F. Browne, N. Fukuda, R. Gemhäuser, G. Gey, N. Inabe, T. Isobe, H. S. Jung, D. Kameda, G. D. Kim, Y.-K. Kim, I. Kojouharov, T. Kubo, N. Kurz, Y. K. Kwon, Z. Li, H. Sakurai, H. Schaffner, K. Steiger, H. Suzuki, H. Takeda, Z. Vajta, H. Watanabe, J. Wu, A. Yagi, K. Yoshinaga, G. Benzoni, S. Böinig, K. Y. Chae, L. Coraggio, A. Covello, J.-M. Daugas, F. Drouet, A. Gadea, A. Gargano, S. Ilieva, F. G. Kondev, T. Kröll, G. J. Lane, A. Montaner-Pizá, K. Moschner, D. Mücher, F. Naqvi, M. Niikura, H. Nishibata, A. Odahara, R. Orlandi, Z. Patel, Z. Podolyák, A. Wendt, *Phys. Rev. C* 91 (2015) 054324.
- [41] P.-A. Söderström, S. Nishimura, Z. Y. Xu, K. Sieja, V. Werner, P. Doornenbal, G. Lorusso, F. Browne, G. Gey, H. S. Jung, T. Sumikama, J. Taprogge, Z. Vajta, H. Watanabe, J. Wu, H. Baba, Z. Dombradi, S. Franchoo, T. Isobe, P. R. John, Y.-K. Kim, I. Kojouharov, N. Kurz, Y. K. Kwon, Z. Li, I. Matea, K. Matsui, G. Martínez-Pinedo, D. Mengoni, P. Morfouace, D. R. Napoli, M. Niikura, H. Nishibata, A. Odahara, K. Ogawa, N. Pietralla, E. Şahin, H. Sakurai, H. Schaffner, D. Sohler, I. G. Stefan, D. Suzuki, R. Taniuchi, A. Yagi, K. Yoshinaga, *Phys. Rev. C* 92 (2015) 051305.
- [42] C. J. Chiara, D. Weisshaar, R. V. F. Janssens, Y. Tsunoda, T. Otsuka, J. L. Harker, W. B. Walters, F. Recchia, M. Albers, M. Alcorta, V. M. Bader, T. Baugher, D. Bazin, J. S. Berryman, P. F. Bertone, C. M. Campbell, M. P. Carpenter, J. Chen, H. L. Crawford, H. M. David, D. T. Doherty, A. Gade, C. R. Hoffman, M. Honma, F. G. Kondev, A. Korichi, C. Langer, N. Larson, T. Lauritsen, S. N. Liddick, E. Lunderberg, A. O. Macchiavelli, S. Noji, C. Prokop, A. M. Rogers, D. Seweryniak, N. Shimizu, S. R. Stroberg, S. Suchyta, Y. Utsuno, S. J. Williams, K. Wimmer, S. Zhu, *Phys. Rev. C* 91 (2015) 044309.
- [43] I. Stefanescu, D. Pauwels, N. Bree, T. E. Cocolios, J. Diriken, S. Franchoo, M. Huyse, O. Ivanov, Y. Kudryavtsev, N. Patronis, J. V. D. Walle, P. V. Duppen, W. B. Walters, *Phys. Rev. C* 79 (2009) 044325.
- [44] S. G. Nilsson, *Kgl. Dan. Vid. Selsk., Mat.-Fys. Medd.* 29 (1955) No. 16.
- [45] D. Pauwels, O. Ivanov, N. Bree, J. Büscher, T. E. Cocolios, J. Gentens, M. Huyse, A. Korgul, Y. Kudryavtsev, R. Raabe, M. Sawicka, I. Stefanescu, J. Van de Walle, P. Van den Bergh, P. Van Duppen, W. B. Walters, *Phys. Rev. C* 78 (2008) 041307.
- [46] S. N. Liddick, S. Suchyta, B. Abromeit, A. Ayres, A. Bey, C. R. Bingham, M. Bolla, M. P. Carpenter, L. Cartegni, C. J. Chiara, H. L. Crawford, I. G. Darby, R. Grzywacz, G. Gürdal, S. Ilyushkin, N. Larson, M. Madurga, E. A. McCutchan, D. Miller, S. Padgett, S. V. Paulauskas, J. Pereira, M. M. Rajabali, K. Rykaczewski, S. Vinnikova, W. B. Walters, S. Zhu, *Phys. Rev. C* 84 (2011) 061305.
- [47] S. N. Liddick, B. Abromeit, A. Ayres, A. Bey, C. R. Bingham, M. Bolla, L. Cartegni, H. L. Crawford, I. G. Darby, R. Grzywacz, S. Ilyushkin, N. Larson, M. Madurga, D. Miller, S. Padgett, S. Paulauskas, M. M. Rajabali, K. Rykaczewski, S. Suchyta, *Phys. Rev. C* 85 (2012) 014328.
- [48] G. Martínez-Pinedo, A. Poves, E. Caurier, A. P. Zuker, *Phys. Rev. C* 53 (1996) R2602.
- [49] N. Shimizu, T. Abe, Y. Tsunoda, Y. Utsuno, T. Yoshida, T. Mizusaki, M. Honma, T. Otsuka, *Progress of Theoretical and Experimental Physics* 2012 (2012) 01A205.
- [50] K. Schreckenbach, P. Liaud, R. Kossakowski, H. Nastoll, A. Bussiere, J. Guillaud, *Physics Letters B* 349 (1995) 427.